ORNL/SPR-2021/1948

Demonstration and Validation of Additively Manufactured Intensified Device for Enhanced Carbon Capture

Costas Tsouris

Gyoung Gug Jang

Josh A. Thompson

Kevin Lai

Xin Sun

Date: March 31, 2021

OAK RIDGE NATIONAL LABORATORY
MANAGED BY UT-BATTELLE FOR THE US DEPARTMENT OF ENERGY

DOCUMENT AVAILABILITY

Reports produced after January 1, 1996, are generally available free via US Department of Energy (DOE) SciTech Connect.

Website www.osti.gov

Reports produced before January 1, 1996, may be purchased by members of the public from the following source:

National Technical Information Service

5285 Port Royal Road

Springfield, VA 22161

Telephone 703-605-6000 (1-800-553-6847)

TDD 703-487-4639

Fax 703-605-6900

E-mail info@ntis.gov

Website http://classic.ntis.gov/

Reports are available to DOE employees, DOE contractors, Energy Technology Data Exchange representatives, and International Nuclear Information System representatives from the following source:

Office of Scientific and Technical Information

PO Box 62

Oak Ridge, TN 37831

Telephone 865-576-8401

Fax 865-576-5728

E-mail reports@osti.gov

Website https://www.osti.gov/

ORNL/SPR-2021/1948

Manufacturing Science Division

FWP-FEAA375
Demonstration and Validation of Additively Manufactured Intensified Device for Enhanced Carbon Capture

SUBMITTED BY

Costas Tsouris, Gyoung G. Jang, Joshua A. Thompson, Canhai Lai, Xin Sun
Oak Ridge National Laboratory
1 Bethel Valley Road
Oak Ridge, TN 37930

PRINCIPAL INVESTIGATOR

Xin Sun, Ph.D.
865 576 3711
sunx1@ornl.gov

Prepared by
OAK RIDGE NATIONAL LABORATORY
Oak Ridge, TN 37831-6283
managed by
UT-BATTELLE, LLC
for the
US DEPARTMENT OF ENERGY
under contract DE-AC05-00OR22725

March 31, 2021

CONTENTS

Figures

Tables

1. SUMMARY

In FY 2018 and 2019, ORNL personnel designed, prototyped, characterized, and tested the enhancement of amine-based carbon capture using additively manufactured *intensified devices*, i.e., devices combining multiple thermodynamic and kinetic processes into one unit operation. State of the art scrubbing technology often employs inter-stage cooling which requires multiple stages of single-purpose unit operations, leading to larger equipment size, higher capital cost, and sometimes less than optimal operating conditions for each piece of equipment. It was proposed that integrating multiple thermodynamic and kinetic operations into one unit could mitigate or negate these drawbacks. Heat and mass transfer studies demonstrated that an additively manufactured intensified device could significantly improve capture efficiency at bench scale. This project is a continuation of FEAA130 and aims at (1) demonstration and validation of enhanced CO_2 capture with 3D printed intensified devices (i.e., mass exchanger packing with internal cooling channels), for low-aqueous-solvent (LAS) based capture at the ORNL-constructed laboratory-scale (4.5-feet tall) column, namely Column A, with built-in cooling and (2) computational scoping on the conceptual design of a flexible and modular larger column, namely Column B, at ORNL for further demonstration of enhanced capture for aqueous solvent. To execute this multi-faceted project scope, an integrated project team from ORNL's Manufacturing Science Division is tasked with applying capabilities in computational fluid dynamics (CFD), additive manufacturing, and absorber-scale demonstration/validation experiments.

As of December 31st, 2020, ORNL researchers successfully completed all milestones of the project FEAA375 by performing absorption-column experiments with low-aqueous amine solvent, and demonstrating that an additively manufactured intensified packing device signficantly enhanced heat and mass transfer. In these experiments, the input solvent temperature was ~40ºC, which is much lower than the 70ºC temperature used for the aqueous MEA solvent. The multifunctional intensified device facilitates contact of the reactive solvent and gas phases in a single stage and facilitates heat removal by a cooling fluid flowing through channels in the interior of the corrugated plates of the device. These functionalities led to effective thermal management along the column via intra-stage cooling and significant improvement in CO_2 uptake under a wide range of operating conditions. Intra-stage cooling effectively reduced the solvent average temperature along the column by ~10°C and, as a result, the solvent's capture efficiency improved by up to 25%.

The ORNL team has also successfully carried out CFD simulations using the MFIX solvent model. The MFIX solvent model is a CFD module developed in NETL's Multiphase Flow with Interphase eXchanges (MFIX) software suite that incorporates basic property data and basic data sub-models to capture the behavior of CO_2 absorbing MEA using the two-fluid model (TFM) approach. The solvent model employs previously validated CFD models with experimental data to investigate and understand these local effects and to generate accurate device-scale models which may result in novel process designs. Using the solvent model, we have first demonstrated that cooling helps to improve the capture efficiency only when the residence time is long enough

and the temperature is high enough. The simulation results using the solvent model, also referencing the results from a process model developed at WVU, contributed to the design of column A. The MFIX solvent model has been used to run simulations to predict the performance of Column A with aqueous amine-based solvents, and the results are compatible with the experimental data. CFD simulations have also been performed to identify the thermal bulge area and to sweep through the realistic design space, i.e., position of the intensified device and desired cooling capability, to identity the optimal location of the intensified device for different operating conditions for larger and taller columns, and this activity has contributed to the design of Column B absorber.

The results of this study demonstrate that intra-stage cooling can be used to enhance carbon capture by as much as 25% at certain process conditions. Intra-stage cooling has been adequately achieved through the additively manufactured ORNL intensified device. Intra-stage cooling may have advantages over inter-stage cooling with respect to capital cost, process footprint, and solvent inventory. Further work is needed, however, to investigate the optimization and scaleup of the intensified device.

2. BACKGROUND INFORMATION

An additively manufactured intensified packing device has been developed at the Oak Ridge National Laboratory (ORNL) in a previous project (FEAA130). The device was subsequently employed to successfully demonstrate CO_2 capture efficiency enhancement using aqueous monoethanolamine (MEA) solutions. In two separate series of experiments, one in which the CO_2 flowrate was varied and another in which the air flowrate was varied to adjust the CO_2 feed concentration at different gas flowrates, the magnitude of the capture rate enhancement was shown to depend on the gas flowrate. Both series of experiments exhibited a peak in the capture rate enhancement at 11.5% at CO_2 concentration of 20% for the CO_2-flowrate varying series and 15.7% at 15% CO_2 concentration for the airflow varying series [Table 1]. The upper range of these data exceeds the performance of *ex situ* inter-cooling predicted in the literature. The overall heat transfer coefficient was found to be in the range of 79–148 W/m^2K. This heat transfer coefficient is near the lower end of the range for plate heat exchangers, which can have heat transfer coefficients ranging from 150 W/m^2K to 15,000 W/m^2K.

Table 1. Improvement in capture efficiency via intensified device using the aqueous MEA solvent. The photo on the left shows the ORNL intensified device developed for the study.

Air Flow Rate (LPM)	CO_2 Flow Rate (LPM)	CO_2 Concentration (%)	Molar Capture Rate Before Cooling (mol/min)	Molar Capture Rate After Cooling (mol/min)	Fractional Increase (%)	Capture Efficiency (%) (Before Cooling → After Cooling)
810	90	10	2.24	2.30	2.7	59.9 → 61.2
510	90	15	2.75	2.90	5.5	73 → 77
360	90	20	2.95	3.29	11.5	78 → 88
264	90	25	3.52	3.57	4.3	94 → 98
360	40	10	1.38	1.45	5.1	83 → 87
360	63.5	15	1.53	1.77	15.7	58 → 67
360	90	20	2.95	3.29	11.5	78 → 88
360	120	25	3.07	3.28	6.9	62 → 66

Solvent flow rate: 3.2 LPM @ 70°C

Solvent-based CO_2 absorption is the most mature technology for CO_2-rich gases, such as the emissions from fossil fuel- and biomass-fired power plants and industrial flue gas streams. Solvent-based CO_2 absorption, however, is also considered one of the most energy-intensive CO_2 capture methods because solvent regeneration requires substantial thermal energy, which is the largest contributor to the process operating cost. A traditional amine-based CO_2 capture solvent (e.g., 30 wt % monoethanolamine [MEA] in water) requires relatively large amounts of thermal energy for heating the solvent during the regeneration process. For example, the reboiler heat duty of aqueous MEA has been estimated to be 3.1–3.75 MJ/kg CO_2.

Toward the reduction of the operating cost, many solvent mixtures such as amine/ammonia-based solvents, nanofluids, water-lean solvents, and nonaqueous solvents have been studied over the past 20 years. An ideal solvent should have high CO_2 absorption capacity, fast reaction rate, low cost, low corrosivity, high thermal and chemical stability, low vapor pressure, and low regeneration heat duty. There are three main contributors to the regeneration heat needed to release CO_2 bonded with amine molecules: (1) the sensible heat (Q_{sen}) required for the solvent to reach the regeneration temperature (e.g., 105°C–110°C), (2) the heat of vaporization (Q_{vap}) for fractional vaporization of the solvent, and (3) the heat of the amine-CO_2 reaction (ΔH_{abs}):

$$Q_{req} = Q_{sen} + Q_{vap} + \Delta H_{abs} \quad (1)$$

The sensible heat and the heat of vaporization can be significantly reduced by replacing water with a low specific-heat capacity and low vapor-pressure solvent. The heat of vaporization depends on the amount of water, which is the largest fraction by weight in CO_2-loaded aqueous amine solutions. A concentrated aqueous-amine solution containing less water and more of a lower–vapor pressure diluent would result in less latent heat of vaporization for the solvent. Several studies have focused on the development of non- or low-aqueous solvents (LASs) to decrease the sensible heat requirement and the heat of reaction. For example, some solvents (e.g., water-lean amine

solvent containing amine result in reboiler duty reduction for regeneration up to 2.0 MJ/kg CO_2, a 40% decrease in duty compared with traditional aqueous solvents.

The LAS studied in this work has lower sensible heat, slightly lower reaction rate between the amine and CO_2, and similar reaction enthalpy compared to aqueous MEA. The primary component of the solvent is a secondary amine. The amine is in a mixture with an organic diluent and a low amount of water (e.g.,<10%) [**Figure 1**]. The LAS has a lower specific heat capacity [i.e., ~2.2 kJ/(kg·K) at 40°C] and heat of vaporization on a mass basis than aqueous MEA [i.e., water C_p = 4.18 kJ/(kg·K) at 40°C]. The kinetics of the secondary amine reaction with CO_2 are slightly slower than the kinetics of the primary amine, MEA, but not significantly enough to impact the absorber height as both are limited by mass transfer in a conventional absorber column. The activation energy of the secondary amine used in the hydrophobic diluent solvent in LAS for the reaction with CO_2 was determined to be 10.37 kJ/mol. The lower water content of the solvent reduces the energy supplied for vaporization of water during regeneration. The amount of water added in LAS also acted as an activator, increasing the reaction rate. Finally, another advantage of LAS is the lower vapor pressure of the solvent, which reduces the solvent heat of vaporization during regeneration and lowers solvent emissions.

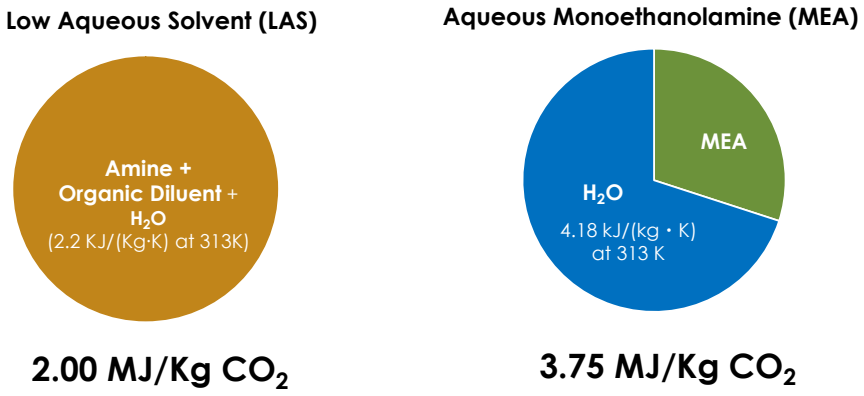

Figure 1. The low aqueous solvent (LAS) and monoethanolamine (MEA) used in this study.

Although LAS has a relatively high re action rate with CO_2 that is desirable for CO_2 absorption, the solvent still requires delicate thermal control because of the heat generated during the reaction. In general, CO_2-amine absorption is an exothermic reaction and releases significant heat (e.g., 80–100 kJ/mol for 30 wt % aqueous MEA solvent at 40°C). The heat released by this exothermic reaction may accumulate in the absorption column, and the bulge temperature along the column can exceed 70°C. Approximately 60% of the absorbed CO_2 desorbs at 90°C, and higher temperatures (100°C or greater) are used for CO_2 desorption and solvent regeneration. The temperature-dependent desorption behavior is favorable for regenerating the solvent; however, it may have a negative effect on the CO_2 capture efficiency when the heat of reaction accumulates in the column. To reduce effects from temperature increase within the absorber, effective interstage cooling using external heat exchangers may be required in a full-scale CO_2 absorption column, increasing the capital and operating costs.

3. CORE METRICS EXPERIMENTAL VALIDATION

3.1 EXPERIMENTAL INFORMATION

3.1.1 Additively Manufactured Intensified Device.

The intensified packing device was designed at Oak Ridge National Laboratory's Manufacturing Demonstration Facility and manufactured by Volunteer Aerospace LLC (Knoxville, Tennessee). The intensified device integrates heat transfer from reactive fluids to a cooling fluid flowing within channels in the interior of the corrugated plates of the packing element and mass transfer between the gas and solvent phases flowing between corrugated plates. These functions of the intensified device are shown in **Figure 2**. The coolant fluid flows around the perimeter of the device and enters spaces within the corrugated plates (baffles). Inside those spaces, the coolant channels run parallel to the corrugation angle so that coolant flows counter-currently with the liquid solvent and co-currently with the gas. Reaction between CO_2 and the solvent occurs within the liquid film on the surface of the corrugated channels, where heat is also released because of the exothermic reaction. The heat is then transferred through the wall of corrugated plates and removed by the coolant flowing through the channels. The inlet and outlet for the coolant are positioned on the sides of the device. The intensified device can be positioned inside the absorption column, preferably near the point where a bulge temperature is expected, to eliminate the need for traditional external heat exchangers, thus reducing complexity and capital and operating costs. The additively manufactured structured packing is also compatible with commercially available structured packing elements that are widely used in gas–liquid or liquid–liquid systems. The final intensified device prototype measures 20.3 cm in diameter, 14.6 cm in height, and the total volume of the internal coolant channels is 600 mL. Aluminum was chosen for its printability and high thermal conductivity.

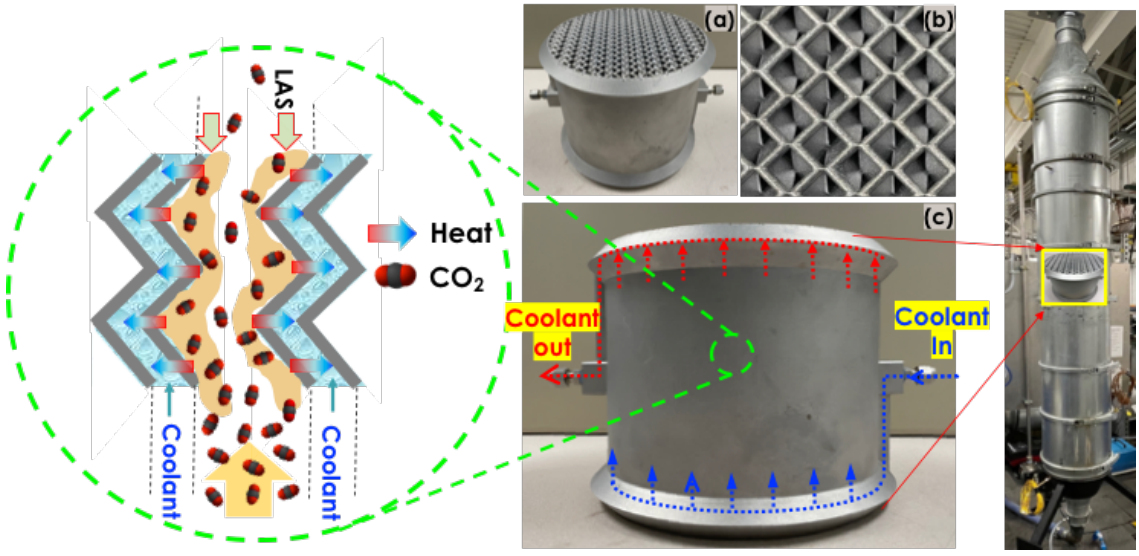

Figure 2. (a) Additively manufactured intensified reactive packing device for CO_2 amine solvent absorption and heat exchange. (b) Top view of corrugated channels for counter current flue-gas scrubbing by the solvent. (c) Front view of intensified device with heat and mass transfer functions.

3.1.2 Testing Facility

An absorption column of 2.06-m height and 0.2-m diameter was operated in a counter-current mode, where LAS was fed to the column from the top and CO_2-rich flue gas entered at the bottom. The column consisted of the intensified packing device and seven stainless-steel Mellapak 250Y commercial packing elements (CPEs) acquired from Sulzer (Winterthur, Switzerland). The intensified device was placed on the top half of the column in the arrangement outlined in Figure 2, with four CPEs located below and three CPEs located above the intensified device. The total bed height occupied by packing elements, including the intensified device, was 1.58 m. The simulated CO_2-rich flue gas was a mixture of air and pure CO_2 at various concentrations. A blower supplied the air at specified flowrates, and the CO_2 came from pressurized gas cylinders. The CO_2 flowrate was set by a Teledyne THCD-101 (Thousand Oaks, California) mass flow controller. The separate streams of air and CO_2 were then mixed and proceeded to enter the absorption column from the bottom. A complete schematic of this experimental system is shown in **Figure 3**.

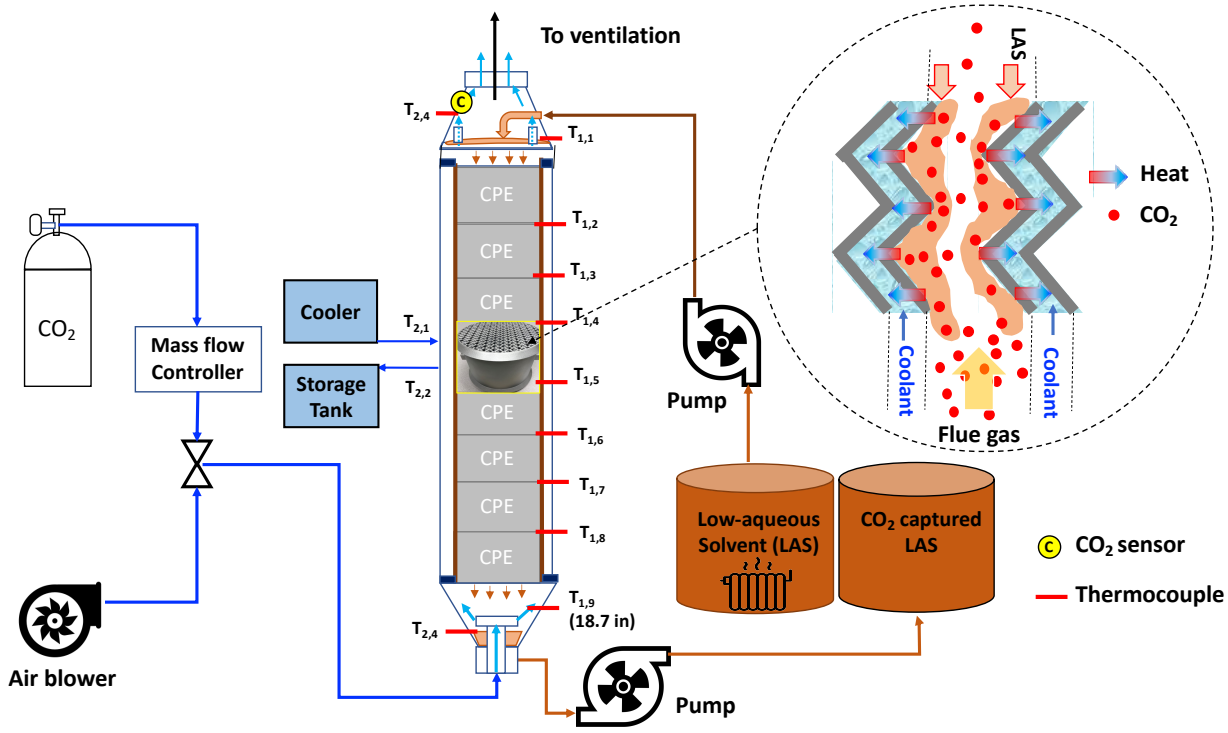

Figure 3. Schematic of Oak Ridge National Laboratory testing facility and CO_2 absorption column.

3.1.3 Experimental Methods

<u>CO_2 Measurement:</u> CO_2 capture efficiency measurements were obtained using a CO_2 meter manufactured by CO_2 Meter (Ormond Beach, Florida). The exit concentration of CO_2 was measured at the top of the column, the exit point for the gas stream. The nominal initial

concentration was determined by the mass flow controller and blower settings; however, it was verified by allowing the gas stream to continue flowing up the column after the solvent stream was cut off and then recording the resulting concentration. The CO_2 capture efficiency was calculated as

$$Capture\ efficiency\ (\%) = \frac{CO_2\ (\%)\ in\ Feed - CO_2\ (\%)\ in\ Output}{CO_2\ (\%)\ in\ Feed} \times 100 \quad (2)$$

Thirteen liquid temperature readings along the height of the column were obtained using type K thermocouples. A time-dependent temperature profile was automatically generated by PicoTech (Cambridgeshire, UK) temperature data recording software at a specified sampling rate of Hz. Geometric temperature profiles were generated by taking the average of the time-dependent temperature profile over 1 min after steady state was reached.

Solvent analysis: The water amount in the LAS was determined by Karl Fischer titration. A CM140 Total Inorganic Carbon Analyzer comprising an Acidification Module CM5330 and a CO_2 Coulometer CM5017 was used to measure the total inorganic carbon in aqueous and organic solutions. The Acidification Module used air as the carrier gas, set to 100 mL/min, which was scrubbed with 45% KOH solution to remove CO_2 from the air. 5 mL of 2 M HCl was added to 0.1–1 mL of sample solution to release CO_2. A scrubber containing 50% KI solution was used to remove H_2S, SO_x, and/or halogens from the resulting mixture of gases that might result from acidification of the samples. Commercially available cathode and anode solutions and KI were used for the CO_2 Coulometer cell.

3.2 MODELING

A simplified equilibrium-stage model was used to compare absorption modeling with the observed column temperature profile for the LAS and to the outlet CO_2 concentration from the experiments. The solubility of CO_2 was determined by a vapor-liquid equilibrium model using a semi-empirical Virial expansion, adopted from Chen and Rochelle, to determine the equilibrium partial pressure of CO_2 based on the loading in the solvent:

$$y^*_{CO_2} P = P^*_{CO_2} = \exp\left(\sum_{j=0} \left(A_j + \frac{B_j}{T}\right) \alpha^j\right) \quad (3)$$

where $y^*_{CO_2}$ and $P^*_{CO_2}$ are the equilibrium mole fraction in the vapor phase and the partial pressure for CO_2 that is in equilibrium with the CO_2 loading in the solvent, α (mol CO_2/mol amine). Water and amine in the solvent were also considered in the absorption modeling, and the ideal Raoult's law was used to determine the equilibrium partial pressure for these components:

$$y^*_i P = P^*_i = x_i P^{sat}_i \quad (4)$$

where x_i is the mole fraction of component i, water or amine, in the solvent and P_i^{sat} is the vapor pressure of component i. The solubility of O_2 and N_2 in the LAS and the vaporization of the organic diluent were assumed negligible.

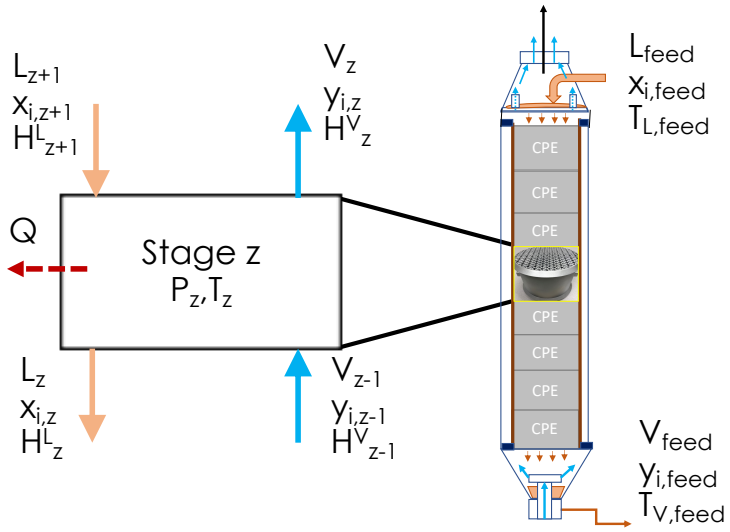

Figure 4. Schematic of equilibrium-stage absorption model with intra-stage cooling.

Figure 4 shows an illustration of the equilibrium-stage model used for the absorption simulations. Because of the absorption column used in the experiments having a fixed number of packing elements, a fixed number of stages equal to the number of packing elements in the experiment, $N_z = 8$, was used in the absorption model.

The overall mass balance in each stage, z, can be written as

$$L_{z+1} - L_z + V_{z-1} - V_z = 0 \tag{5}$$

where L and V are the total liquid and vapor molar flowrates, respectively. The component material balances are

$$x_{i,z+1}L_{z+1} - x_{i,z}L_z + y_{i,z-1}V_{z-1} - y_{i,z}V_z = 0 \tag{6}$$

The energy balance is determined by

$$h_{L,z+1}L_{z+1} - h_{L,z}L_z + h_{V,z-1}V_{z-1} - h_{V,z}V_z + \Delta H_R - \Delta H_{vap,H_2O} - \Delta H_{vap,am} - Q = 0 \tag{7}$$

where h_L and h_V are the enthalpies of the vapor and liquid, respectively, ΔH_R is the heat of reaction generated at each stage by CO_2 absorption into the solvent from the vapor, $\Delta H_{vap,i}$ is the heat of vaporization generated by water and amine at each stage, and Q is the heat loss during cooling experiments at the stage containing the additively manufactured structured packing. The heat of reaction is the summation of the CO_2 dissolution into the solvent and reaction with the amine. The heat of absorption for CO_2, which may be assumed as the heat generated by the reaction with

amine, was determined using the Gibbs-Helmholtz equation for the semi-empirical Virial solubility model:

$$\Delta H_{abs} = -R \frac{d \ln P}{d\, {}^{1}/_{T}} = -R \sum_{j=0} \left(B_j\right) \alpha^j \tag{8}$$

The heat of dissolution was assumed to be equivalent to CO_2 dissolution in water. Because water was used as the coolant in the cooling experiments, the heat loss may be determined by

$$Q = m_{H_2O} \int Cp\, dT \tag{9}$$

where m_{H_2O} is the mass flowrate of water, and C_p is the heat capacity.

The nonideal behavior in absorption columns was approximated by assuming a stage efficiency. To simplify the model, a universal stage efficiency was assumed for each simulation, and the Murphree efficiency equation was used to determine the vapor-phase mole fraction for component *i* at stage *z*:

$$ME_z = \eta_z = \frac{y_z - y_{z-1}}{y_z^* - y_{z-1}} \tag{10}$$

A range of 30% to 90% stage efficiency was used to compare the range of model prediction with the experimental data.

3.3 RESULTS AND DISCUSSION

3.3.1 Enhancement of CO_2 capture efficiency

A series of experiments showed significant improvement in the CO_2 capture by the intensified structure packing device. The fractional percentage increase in the capture rates ranged from 4.3% to 25.1% depending on operational conditions as shown in **Table 2**.

The feed solution temperatures were studied between 40°C and 60°C considering the broad range of practical operational conditions. The relatively short height of the absorption column (1.58 m) presented a challenge for studying the intra-stage cooling effect by the intensified device using aqueous MEA because the solvent residence time was not long enough to sufficiently heat the column. The height of a practical packing material in a commercial absorption column is considered to be 25–40 m. For this reason, in previous work, the solvent (30 wt % aqueous MEA) was heated to 70°C prior to entering the column. However, we observed that the LAS during the experiments shown in Table 2 was more sensitive to temperature compared with aqueous MEA. For example, with a LAS feed temperature of 40°C, the heat generation from the CO_2-LAS absorption reaction and the heat accumulation along the column was enough to impact the CO_2 capture efficiency. Note that the capture enhancement for LAS was much higher than that for the aqueous MEA at similar operating conditions [**Figure 5**].

Table 2. Improvement in CO_2 capture efficiency by intra-stage cooling using the intensified packing device. The local temperatures along the column height were measured by eight thermocouples, and average measurements at the steady state were determined before and after cooling.

Exp	Solvent Condition	Solvent Flowrate (LPM)	Air flowrate (SLPM)	CO_2 flowrate (SLPM)	CO_2 Amount (%)	CO_2 output before cooling (%)	CO_2 output after cooling (%)	Capture efficiency (%) (before → after)	Fractional Improvement (%)*	Feed temp. (℃)	Average temp.	
											No-cooling	Cooling
1	Pristine	3.26	510	90	13.8	2.21	0.64	84 → 95.4 (11.4↑)	13.5	59	60.7	52.2
2	Pristine	3.26	510	90	14.0	1.95	0.47	86 → 96.6(10.6↑)	12.3	52	59.6	50.4
3	Pristine	3.26	510	90	13.8	1.61	0.64	88.3 → 95.4 (7.1↑)	8.0	45	58.6	50.0
4	1st Regen.	3.26	510	90	14.7	3.18	1.57	78.4 → 89.4(11.0↑)	14.0	41	54.5	45.3
5	2nd Regen	3.26	608	107	13.1	3.75	2.23	71.3 → 82.9(11.6↑)	16.3	44	55.2	46.8
6	2nd Regen + DI H_2O(5L)	3.26	608	107	13.0	2.94	2.08	77.4 → 84.0(6.6↑)	8.5	44	55.4	46.9
7	3rd Regen	3.26	425	75	13.3	1.19	0.67	91.1 → 95.0(3.9↑)	4.3	41	52.8	44.9
8	3rd Regen	2.82	510	90	13.1	2.75	1.75	79.1 → 86.7(7.6↑)	9.7	41	53.8	46.6
9	4th Regen	3.26	353	62	13.3	0.79	0.44	94.0 → 96.6(2.6↑)	2.8	41	49.8	39.7
10	4th Regen	3.65	510	90	12.8	2.16	1.13	83.2 → 91.2(8.0↑)	9.7	41	52.7	44.2
11	5th Regen	2.39	510	90	13.1	5.85	4.71	55.3 → 64.0(8.7↑)	15.7	41	52.3	45.5
12	5th Regen	2.82	510	90	13.0	4.92	3.25	62.2 → 75.0(12.8↑)	20.7	41	54.2	46.4
13	6th Regen	3.26	510	90	13.2	5.74	3.86	56.7 → 70.9(14.2↑)	25.1	41	53.5	45.0
14	6th Regen + DI H_2O(5L)	3.26	510	90	13.1	5.33	4.73	59.3 → 63.9(4.6↑)	7.8	41	52.1	43.5

(a)	MEA	LAS
Feed temperature (℃)	70	**40**
Avg. Temperature **before cooling**	72.0 ± 9.9 (n=4)	**54.5** ± **5.5** (n=8)
Avg. Temperature **after cooling**	60.5 ± 13.9 (n=4)	**45.3** ± **6.8** (n=8)

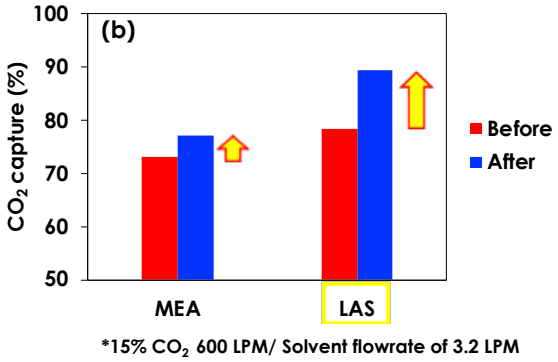

Figure 5. (a) Average temperature comparisons between Aqueous MEA and LAS before and after cooling. (b) Corresponding CO_2 capture efficiency enhancement.

3.3.2 Thermal management by intra-stage cooling

Time-dependent CO_2 concentration profiles before and after intra-stage cooling by the intensified packing device were measured as shown in **Figure 6**a. The absorber was operated in a counter-current mode in which CO_2-lean LAS was fed to the top of the column while CO_2-rich flue gas (~14%) was fed to the bottom. As CO_2 was absorbed by the LAS, the temperature of the solvent increased as shown in Figure 6b. Initially, the CO_2 concentration rapidly dropped at the gas outlet as the entire column was still cold because of the amine-CO_2 absorption reaction. Column temperature measurements along the axial direction, except for the top ($T_{1,1}$), increased to

50°C or greater after 300 s. Following the observed column temperature increase, the CO_2 concentration at the gas outlet gradually increased and reached an approximate steady-state value of 1.95% for the experiment shown in Figure 6a. Subsequently, the column temperatures reached an approximate steady state (e.g., $T_{1,3}$ at 63.5°C) at 700 s of operation before cooling was introduced to the column. When water coolant at 8°C was introduced through the intensified device, the temperatures of the column rapidly decreased and reached a second steady state around 900 s. At this new steady state, the CO_2 outlet decreased from 1.95% to 0.47%, and the observed column temperatures above and below the intensified device, namely $T_{1,4}$ and $T_{1,5}$, decreased significantly from approximately 60°C to 40°C. Once sufficient time was allowed for this new steady state to be reached, the flow of solvent was stopped, while CO_2 gas concentration measurements at the exit and temperature measurements along the column continued. The data presented in Figure 6 are representative of other experiments summarized in Table 2.

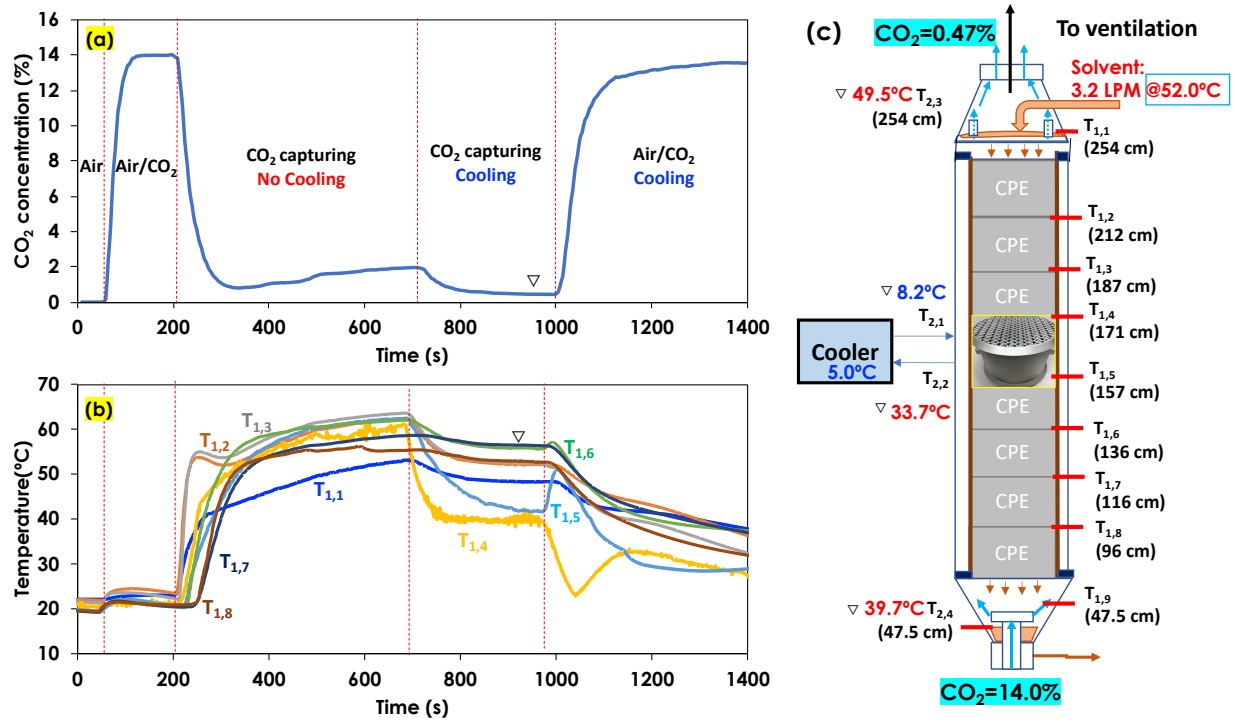

Figure 6. (a) Time-dependent CO_2 concentration profile during CO_2 absorption by the LAS with intra-stage cooling. The LAS process was tested at 600 LPM gas flowrate and 14% CO_2 feed concentration at ~50°C, with the LAS feed at 3.2 LPM. (b) Corresponding time-dependent temperature profiles along the column. (c) Schematic of column with the CO_2 concentration and temperature measurements at steady state with intra-stage cooling. The reverse triangles in (a) and (b) indicate the points in time at which steady-state data for experiment 2 were recorded in Table 2.

Figure 7a demonstrates that the intensified packing device located at the middle of the column between $T_{1,4}$ and $T_{1.5}$ may supply sufficient cooling to the entire column. The temperature profiles along the column showed a pronounced temperature bulge at the midpoint of the column under adiabatic conditions. Because of the intensified device located at the midpoint, the temperature

profile was slightly lower than either above or under the column midpoint when the intensified packing was loaded with coolant. The temperature bulge location could be varied by the operational conditions, such as solvent and gas flowrates, solvent composition, height of packing and CO_2 concentration in the flue gas. Once intra-stage cooling started, a significant temperature drop was observed near the intensified device, as well as in the entire column, demonstrating effective cooling by the intensified device and an average of 9.2°C temperature reduction along the column. Thermal management through intra-stage cooling resulted in improved CO_2 capture efficiency, decreasing the outlet flue gas CO_2 concentration and reaching a steady state of 0.47% at 950 s in Figure 7b. The corresponding capture efficiency increased from 86.0% to 96.6%, representing a fractional increase of 12.3% (Table 2).

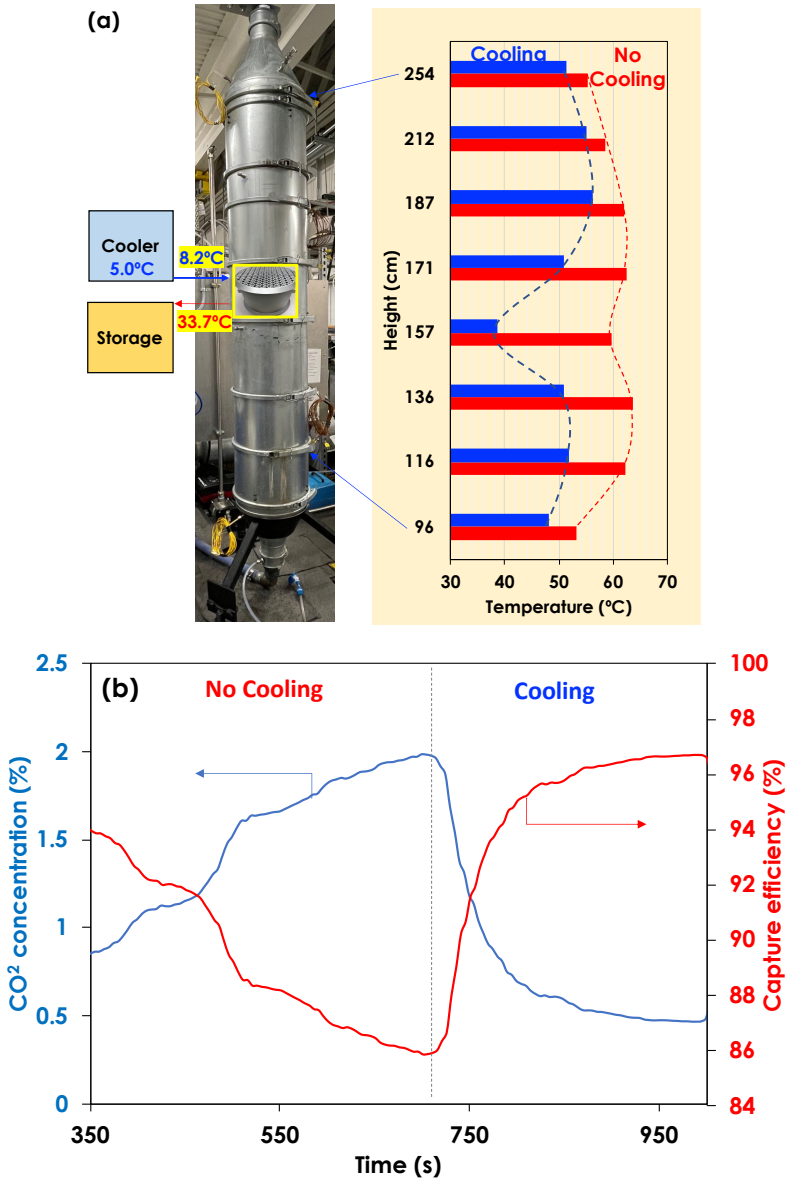

Figure 7. (a) Axial steady-state temperature profile along the column height before and after intra-stage cooling. (b) Time-dependent profiles of CO_2 concentration and CO_2 capture efficiency during experiment 2 (Table 2).

3.3.3 Effects of operating parameters on CO_2 capture enhancement

Various operating conditions were tested to evaluate the CO_2 capture improvement using the intensified device. The CO_2 outlet concentration versus inlet solvent temperature in **Figure 8**a suggests that the CO_2 capture efficiency by the LAS depends on the solvent temperature within the absorption column. As the solvent feed temperature decreased from 58°C to 52°C to 45°C, the CO_2 concentration at the gas exit decreased from 2.2% to 2.0% to 1.6%, respectively, at a steady state prior to cooling. After cooling, the CO_2 outflow concentrations further decreased to 0.4%–0.6%, resulting in fractional improvement in CO_2 capture efficiency of 13.5%, 12.0%, and 8.0%, respectively. The steady-state local temperature profiles for $T_{1,3}$ and $T_{1,6}$, as shown in Figure 8b, indicate that these temperatures dropped between 5°C and 12°C, a behavior correlated with the capture efficiency improvement. The position of $T_{1,3}$ and its magnitude suggest the highest heat accumulation at that point for the specific operating conditions of experiments 1–3 (Table 2). The highest fractional capture improvement occurred when the hottest axial position within the column was cooled to 55°C from 65°C. These experiments were carried out with pristine LAS, and subsequent experimental sets were tested using regenerated LAS at 105°C.

Similar to studies using aqueous MEA, higher ratios of liquid-to-gas (L/G) mass flowrates favor higher capture efficiency of CO_2, resulting in a trade-off between lower CO_2 outlet concentrations and increasing solvent flowrate relative to gas flowrate (Figure 8c). Intra-stage cooling further improved the capture efficiency. In the experiments shown in Figures 8c and d, the liquid flowrate increased while the gas flowrate was fixed at 600 LPM (or 0.77 kg/min). Similar to other experiments, the effect of intra-stage cooling shown in Figure 8d contributed to an increase in the CO_2 capture efficiency as shown in Figure 8c. Figure 8e shows that increasing the L/G ratio reduced the CO_2 outlet concentration, which is consistent with observations in Figure 8c. In the experiments shown in Figure 8e and f, the incoming gas flowrate was decreased while the liquid flowrate was kept constant at 3.26 LPM. Because of a lower incoming CO_2 mass flowrate, the overall capture efficiency increased with increasing L/G, and heat accumulation decreased as observed by changes in the column temperature profile for $T_{1,3}$ and $T_{1,6}$. Although the local heat accumulation was relatively small (e.g., at L/G = 6.1 in Figure 7e and f) at 45°C–47°C, intra-stage cooling through the intensified device demonstrated an improvement of approximately 3% in the CO_2 capture efficiency by further reducing the temperature. These data suggest that the optimal temperature conditions during CO_2 absorption by LAS may be below 45°C.

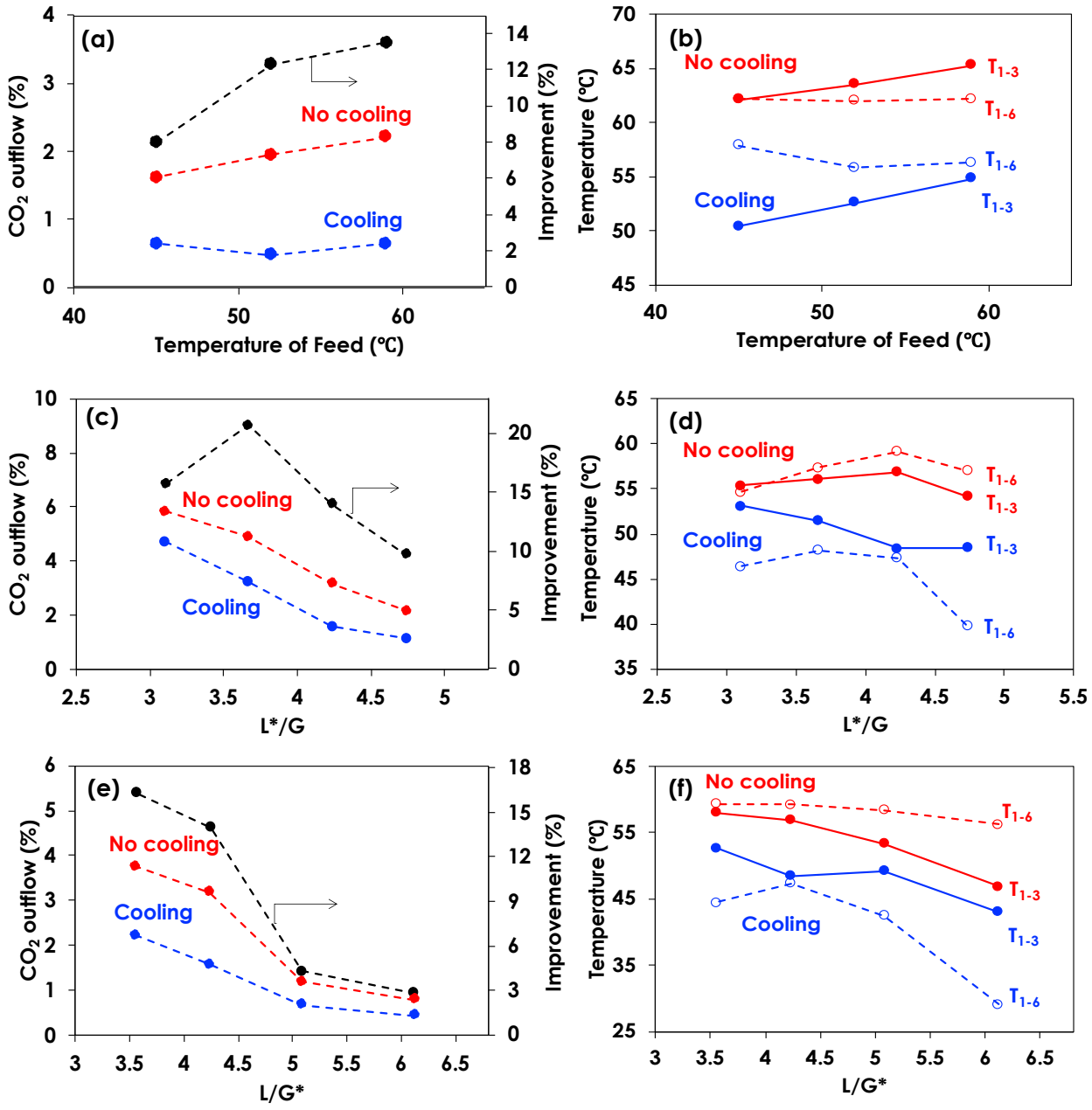

Figure 8. (a) Feed temperature effects on CO_2 capture efficiency. The simulated flue gas operating conditions are 13% CO_2 with L/G = 4.2. Results are from experiments 1, 2, and 3 in Table 2. (b) Corresponding local steady-state temperature profiles. (c) Liquid solvent flowrate effects (L*) on CO_2 capture efficiency. The flue gas flowrate (13% CO_2) was fixed at 600 LPM and the temperature of the feed solution was at 41°C. Results are from experiments 4, 10, 11, and 12 in Table 2. (d) Corresponding local steady-state temperature profiles. (e) Gas flowrate effects (G*) on CO_2 capture efficiency. The temperature of the feed solution was 41°C and LAS flowrate was 3.26 LPM. Results are from experiments 4, 5, 7, and 9 in Table 2. (f) Corresponding local steady-state temperature profiles.

3.3.4 Regeneration effects on CO_2 absorption performance

A CO_2 desorption profile shown in **Figure 9** was determined by heating the CO_2-rich LAS for regeneration and monitoring both the gas-phase CO_2 concentration and inorganic carbon content of the solvent. The concentration (percentage of CO_2 in gas) of the released CO_2 was determined using the CO_2 gas detector. Because of the limit of detection being within 0%–32% CO_2 concentration, measurements above 85°C were not possible, but solvent measurements revealed that CO_2 desorption started at 50°C, indicating that LAS is sensitive toward temperature changes. The unique kinetic and equilibrium behavior may explain why intra-stage cooling by the intensified device was effective on CO_2 absorption enhancement for this LAS formulation at intermediate feed temperatures of 40°C–60°C. For all experiments, we observed that the column was quickly heated to 50°C–60°C by the solvent before intra-stage cooling was activated. At such temperatures, based on the desorption profile shown in Figure 8, unfavorable desorption or reduced mass transfer may occur within the absorption column. The concentration profile from dissolved CO_2 concentration in the CO_2-rich LAS indicates that sufficient regeneration occurred at 105°C, with approximately 0.5 gC/L concentration remaining in the CO_2-lean solvent.

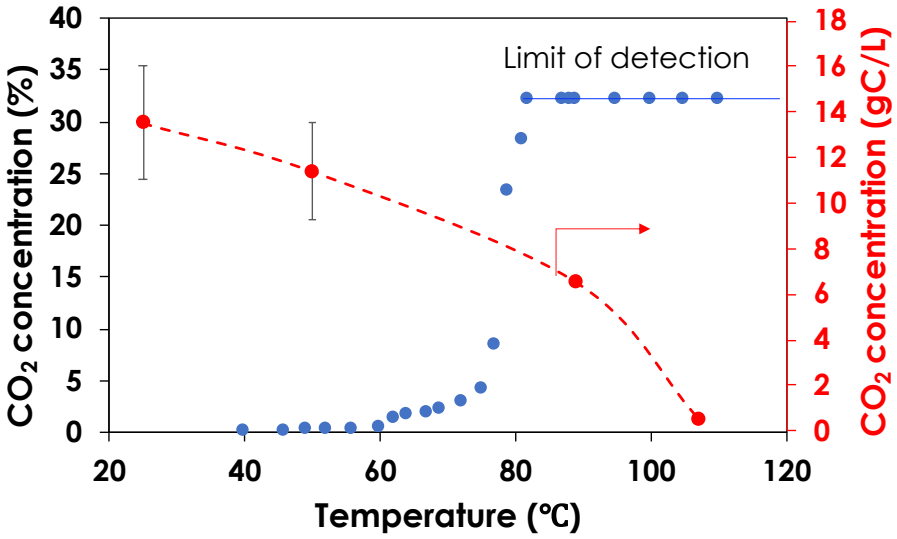

Figure 9. Temperature effect on regeneration of CO_2-rich LAS.

After repeating the regeneration process (i.e., at 105°C for 30 min), the CO_2 capture efficiency decreased as shown in **Figure 10**a. The regeneration profiles related to the capture efficiency were examined based on selected operating conditions, including L/G = 4.2 at a fixed liquid flowrate of 3.26 LPM and 41°C feed solvent temperature. For the 3rd and 5th regenerations, a solvent flowrate of 2.82 LPM was selected for comparison. Based on total inorganic carbon analysis and water content, as shown in Figure 10b, the composition of the regenerated CO_2-lean LASs may have contributed to the observed decrease in CO_2 capture performance. The remaining CO_2 in the lean solvent after regeneration may have significantly affected the mass transfer driving force for CO_2 capture. The steady-state temperature profiles shown in Figure 10c for the no-cooling and cooling

states indicate that the accumulated heat along the column was also significantly reduced in combination with the capture efficiency reduction after the first and subsequent solvent regenerations. The lower heat accumulation implies that the rate and extent of the exothermic CO_2 gas-liquid reaction after regeneration may have decreased relative to the pristine LAS.

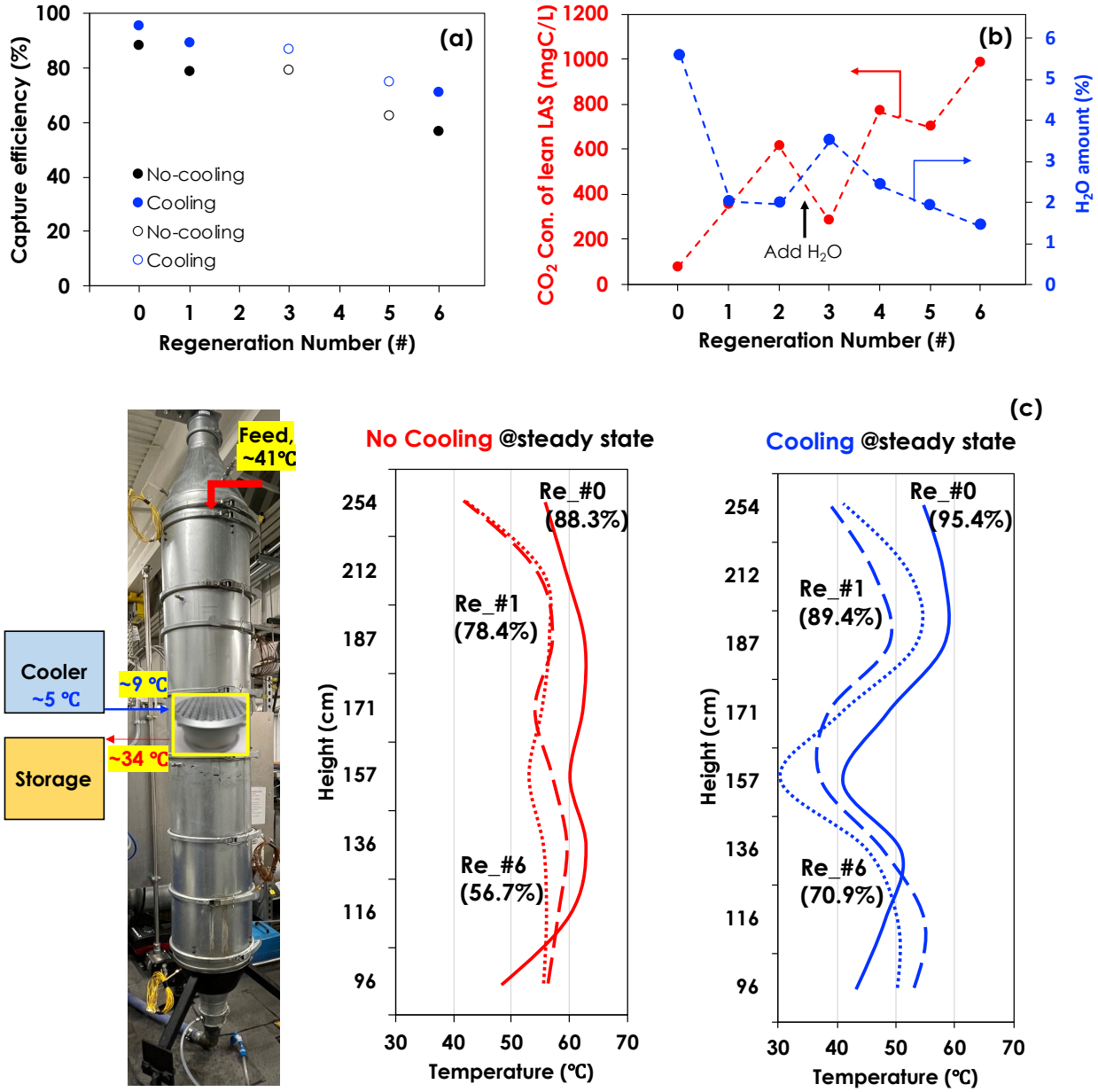

Figure 10. (a) CO_2 capture efficiency of the LAS after multiple regenerations. The solid circles indicate the results of experiments 3, 4, and 13 that were tested for pristine solvent and after regenerations 1, and 6, whereas the empty circles indicate the results of experiments 8 and 12 after regenerations 3 and 5. (b) Corresponding CO_2 and H_2O concentrations in the CO_2 lean LAS after regeneration at 105°C for 30 min. (c) Temperature profiles of no cooling/cooling during CO_2 absorption. (Re_# stands for the regeneration number.)

After six regeneration cycles, the CO_2 concentration of the lean solvent reached approximately 1 g C/L solvent, corresponding to the lowest capture efficiency for the lean solvent. In addition to the concentration of CO_2 in the lean solvent, the presence of water in the LAS may be another factor contributing to the performance of the solvent in CO_2 absorption/desorption. Previous work has reported that water in the LAS acts as an activator to increase the reaction rate with CO_2. The optimal water concentration in the LAS that keeps the solvent activated and the regeneration rate low is at 5%. Addition of deionized water (5L) to the storage tank (~95 L of the LAS) before the 3rd regeneration was used to understand the water activation effect. The water amount in the regenerated LAS, shown in Figure 10b, increased after the water addition while the remaining CO_2 amount in the lean solvent significantly decreased after the regeneration. Following this behavior, the regeneration was repeated without further addition of water to understand the efficacy of the added water for removal of CO_2 concentration in the lean solvent after multiple regenerations. The role of water and amine content will be further studied in future work to optimize the regeneration efficiency and its effect on the CO_2 capture process with LAS.

Table 3. Characteristics of the LAS in CO_2 absorption and water content after capture and regeneration. The operating conditions include constant CO_2 feed rate (13%, 600 LPM) with 3.26 LAS flowrate. * indicates the absorption value was determined by CO_2 gas measurement.

Experiment		#1	#2	#3	#4	#13		#14	
Operation		Cooling	Cooling	Cooling	Cooling	No-cooling	Cooling	No-cooling	Cooling
Feed LAS	CO_2, gC/L		0.076		0.351	0.987		0.934	
	[H_2O,%]		[5.56]		[2.01]	[1.42]		[7.59]	
Outflow LAS	CO_2, gC/L	12.89	11.38	16.28	8.07	9.50	9.63	12.98	13.58
	[H_2O,%]	[3.25]	[1.90]	[2.00]	[1.65]	[0.81]	[0.71]	[5.33]	[5.98]
CO_2 absorption (gCO_2/L, liquid basis)		47.0	41.4	59.4	28.9	31.2	31.7	44.2	46.4
CO_2 absorption* (gCO_2/L, gas basis)		51.3	52.0	51.3	48.1	30.4	38.09	31.9	34.4

Table 3 shows the dissolved CO_2 and water concentrations in LAS samples before and after intra-stage cooling. The dissolved CO_2 analysis in the solvent was correlated with the observed CO_2 absorption results determined by CO_2 concentration at the inlet and outlet of the gas used in the experiments. The mass balance results based on the dissolved CO_2 in the liquid solvent samples are within 2%–40% of the gas basis for CO_2 absorption amount determined by the gas-phase measurement of CO_2. When intra-stage cooling was used, there was a higher degree of absorption for CO_2 compared with adiabatic conditions in the column, and this was also correlated with the

dissolved CO_2 concentrations shown in Table 3 for experiments 13 and 14. Because of changing CO_2 and water concentrations in the CO_2-lean LAS, comparing the experimental data for different regeneration cycles is difficult. The effect of water, amine content, and lean CO_2 concentration will be further studied in future work to better understand and optimize the CO_2 capture process using LAS.

3.3.5 LAS Modeling

Two modeling approaches may be used for estimating the absorber performance for removal of CO_2: equilibrium-based models and rate-based models. Rate-based models have shown accurate prediction of the behavior for aqueous amine solvents for flue gas carbon capture absorption conditions given that mass transfer from the flue gas to the solvent can depend on reaction within the liquid phase. To properly account for rate-based modeling methods, the reaction kinetics between CO_2 and the amine solvent, the mass transfer between gas and liquid phases, and the vapor-liquid equilibria must be described accurately. Therefore, these modeling approaches may be computationally intensive or require commercial process simulation software as well as detailed physical and transport properties for the solvent. Equilibrium-based models assume liquid and vapor leaving a stage within a packed column are in equilibrium with each phase, and this assumption includes chemical, thermal, and mechanical equilibria. Only the CO_2 solubility and physical properties of the solvent are needed to estimate the absorption using an equilibrium-based modeling approach, reducing the complexity of the simulations. However, this approach may not necessarily be used a priori to design a new absorption column or transfer models to different operational scales, but these simulation tools may be useful in understanding the observed experimental behavior of a given solvent for removing CO_2 from flue gas.

To further simplify the equilibrium-based model, a semi-empirical solubility model for the LAS-CO_2 system was used based on a previously published semi-empirical model from Chen and Rochelle. The model may be used to describe equilibria of CO_2 between flue gas and LAS in an absorption column, but this model cannot describe changes in CO_2 solubility with variations in the solvent formulation. **Figure 11** shows the parity plot demonstrating how well this model describes the prediction of the equilibrium CO_2 partial pressure. Although there is generally good prediction of the equilibrium partial pressure below 1 bar for the entire temperature range, there is considerable deviation at the higher partial pressures, which are not relevant for the absorber conditions considered in CO_2 capture experiments. Further work to develop vapor-liquid equilibrium (VLE) models, such as electrolyte-NRTL or Pitzer activity-based models, may provide more accuracy and account for changes in the composition of the main constituents of the solvent.

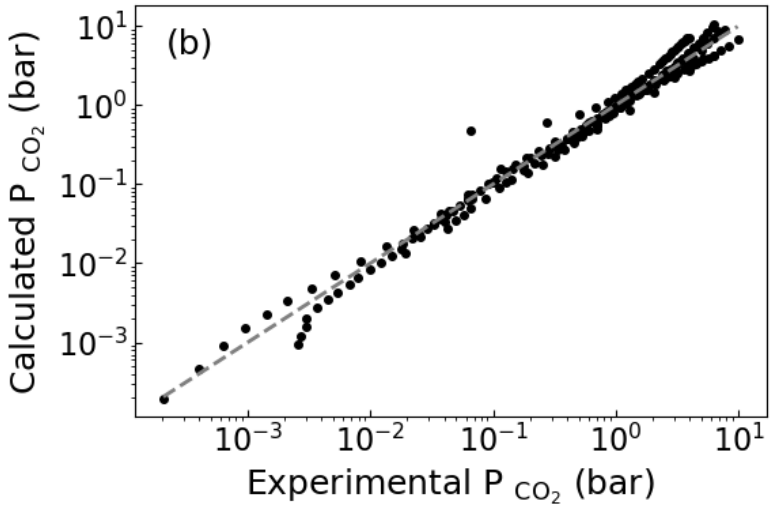

Figure 11. Parity plot of experimental CO_2 equilibrium partial pressure with calculated partial pressure from the Virial model.

Following the simulation methodology described previously, simulations of absorption experiments were performed to compare predictions of the equilibrium-based absorption model with experiments before and after intra-stage cooling. The improvement in CO_2 capture with the additively manufactured structured packing may be understood by examining a McCabe-Thiele plot comparing the operating and equilibrium lines before and after cooling in the device. **Figure 12** shows the calculated operating and equilibrium lines for experiment 1 (Table 2) and 90% stage efficiency, calculated based on the stage temperature and composition from the absorption simulation. When there was no cooling within the absorption column, a near-pinch between the operating and equilibrium lines reduced the amount of CO_2 removed within these stages. Once cooling was applied, the area between the operating and equilibrium lines increased, resulting in the observed process intensification when cooling was applied in the experiment.

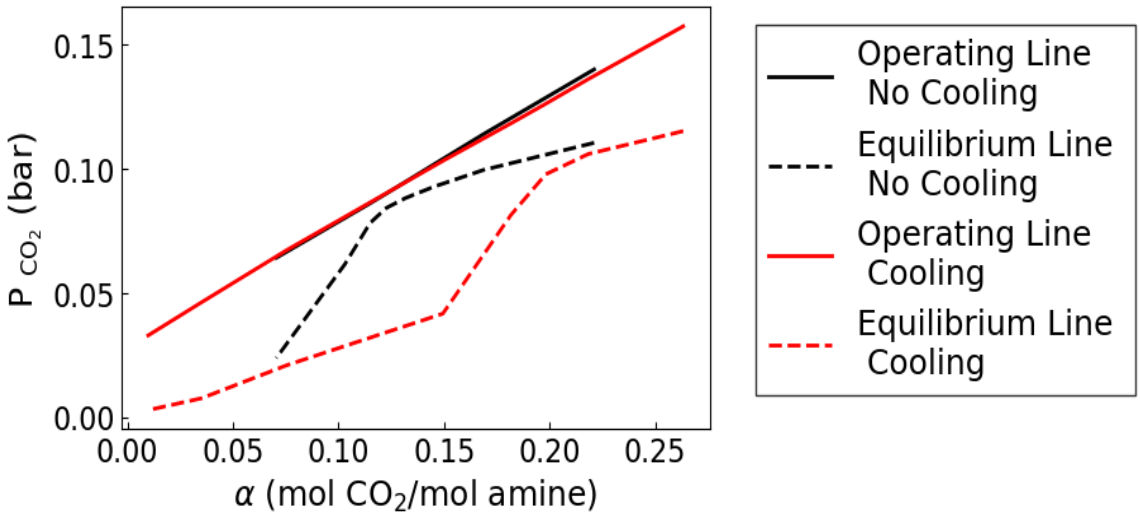

Figure 12. McCabe-Thiele plot of operating (solid) and equilibrium (dashed) line for the absorber with experiment 1 conditions before (black) and after (red) cooling with 90% stage efficiency.

Equilibrium-based simulations of experiments 1–3 were performed based on experimental conditions from Table 2. These experiments used the pristine LAS and would be best described by the solubility model above because no regeneration had been applied to the solvent. Given the pristine solvent used in these experiments, the lean CO_2 loading was assumed negligible in simulations. All simulations were performed using an algorithm developed in Python, and physical property data, such as heat capacity, heat of vaporization, and heat of formation, were obtained from Design Institute for Physical Properties (DIPPR) or Aspen Properties if available. **Figure 13** shows the temperature profile and the predicted CO_2 profile compared with the measured temperatures and the inlet and outlet CO_2 concentrations for experiment 1 before and after cooling. Prior to cooling, the simulations under assumption of adiabatic conditions showed good agreement between the measured temperature profile and simulations that assume a stage efficiency of 60% or greater. However, the CO_2 removal predicted by the simulations under adiabatic conditions (Figure 13a) did not adequately match the experimental data at lower stage efficiencies despite the agreement with the temperature profile (Figure 13c). Only at a stage efficiency of 90% or greater did the simulation and experiment show agreement for the CO_2 outlet concentration. This was also observed in simulations of experiments 2 and 3. The stage efficiency in these simulations served as an empirical means to account for effects of mass and heat transfer and reaction kinetics that can alter the absorption behavior. The high stage efficiency necessary to predict both an accurate temperature profile and CO_2 outlet concentration under adiabatic conditions suggests the solvent may not show the same rate limitations that aqueous amine solvents show.

With intra-stage cooling applied within the device, there is an increase in the amount of CO_2 removed by the solvent compared with adiabatic conditions shown by both the experiments and simulations. In Figure 13b, the CO_2 profiles from the simulations between a stage efficiency of 60% and 90% agree with the observed CO_2 outlet concentration in the experiment. The temperature profiles shown in Figure 13d suggest that at higher stage efficiency (where more mass transfer of CO_2 from the gas phase to the liquid phase occurs), the cooling in the additively manufactured device had less of an effect on the stage temperature, possibly because of the increased heat generated by CO_2 absorption. Stages before and after cooling showed agreement between experimentally observed temperature profile and simulations between 60% and 90% stage efficiency. Because the heat removed by cooling was calculated based on the measured temperature of the coolant entering and leaving the packing, there is a limited range of temperature reduction within the packing at these higher stage efficiencies. Further simulation work to understand the individual enthalpic effects, such as heat of absorption or heat of vaporization, on the calculated temperature profile under adiabatic and cooling conditions may provide improved understanding on the CO_2 capture process using simulations. This would require more experimental data to better estimate the effect of solvent composition on the vapor-liquid equilibria as well as other thermodynamic properties of the solvent.

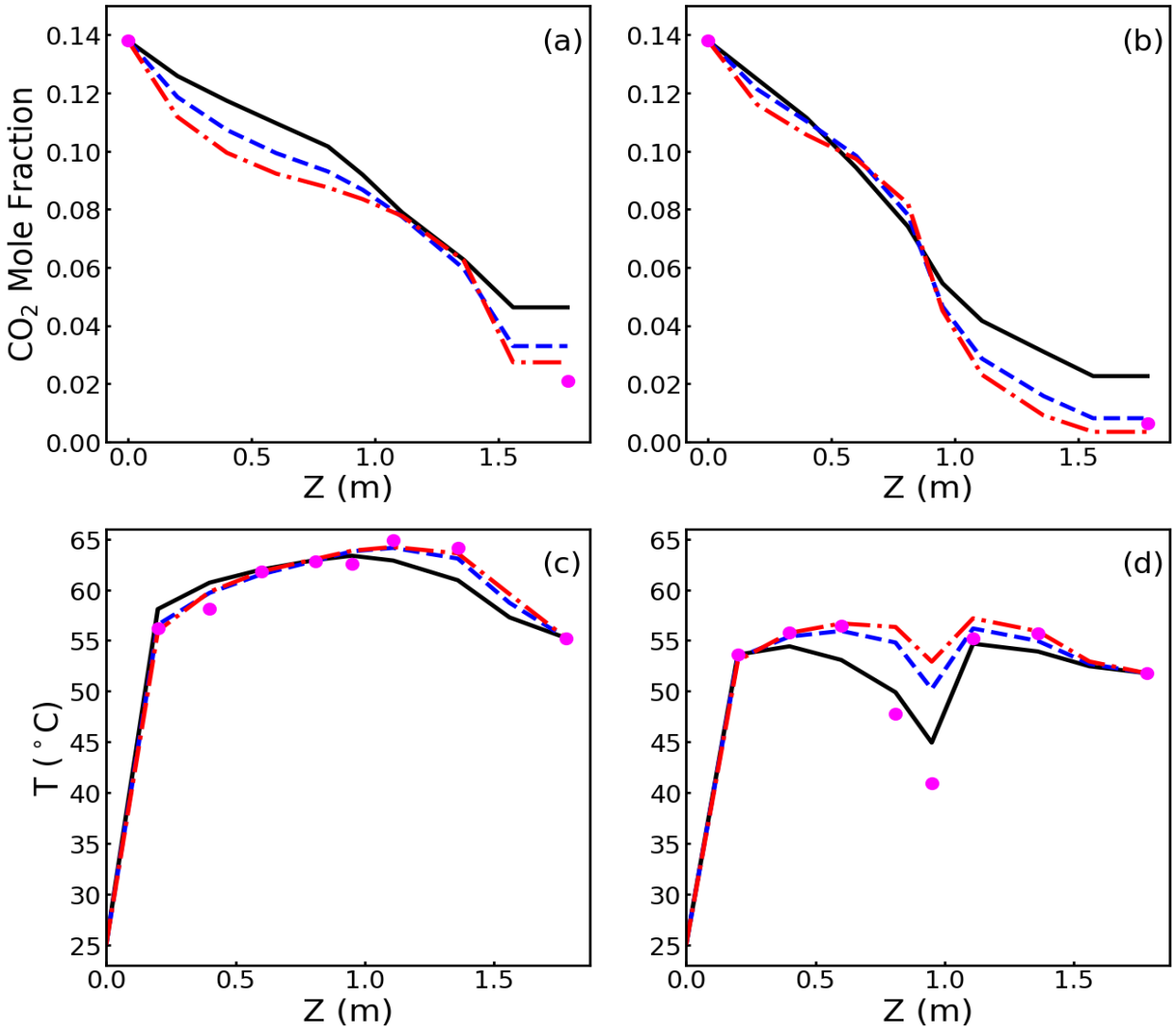

Figure 13. CO_2 concentration profiles along the absorption column (a) before and (b) after cooling; and temperature profiles along the absorption column (c) before and (d) after cooling. Symbols are from experiment 1, and lines are from different simulations varying the stage efficiency at 30% (black, solid), 60% (blue, dashed), and 90% (red, dash-dot).

4. DEVICE SCALE VALIDATION THROUGH DESIGN OF EXPERIMENTS

4.1 MODELING

The MFIX solvent model used in this task is a CFD module developed in NETL's Multiphase Flow with Interphase eXchanges (MFIX) software suite that incorporates basic property data and basic data sub-models to capture the behavior of CO_2 absorbing MEA using the two-fluid model (TFM) approach. The solvent model employs previously validated CFD models with experimental

data to investigate and understand these local effects and to generate accurate device-scale models which may result in novel process designs.

Using the solvent model, we have first demonstrated that cooling helps to improve the capture efficiency only when the residence time is long enough and the temperature is high enough. This phenomenon can be explained by the facts that higher temperature increases chemical reaction kinetics but the equilibrium tilts toward the reverse reactions if the temperature is too high, and the longer residence time allows the reaction to reach the equilibrium. This finding is consistent with the prediction by the AspenPlus based model developed at the West Virginia University (WVU). The results from the processed model and MFIX simulations agree qualitatively in terms of the effect of cooling on the CO_2 capture. Results from the earlier parametric study using the solvent model have helped the design of the current column (Column A) including geometry, cooling configuration, and inlet conditions such as flowrates and temperature.

The MFIX solvent model has been used to run simulations to predict the performance of Column A with aqueous amine-based solvents, and the results generally matched well the experiment data. Table 4 recaps the comparison of CO_2 capture in several experimental tests for Column A. All simulations followed the experimental setup, geometry, and the boundary conditions as much as possible. Column A was first used for thermal experiments, i.e., without any CO_2 in the gas, and later with CO_2 and thus the capture reactions in the column. The insulation for Column A has improved over time and, as a result, non-adiabatic simulations were performed first and adiabatic ones were run later.

CFD simulations have also been performed to identify the thermal bulge area and to sweep through the realistic design space, i.e., position of the intensified device and desired cooling capability, to identity the optimal location of the intensified device for different operating conditions for larger and taller columns, and this activity has contributed to the design of the Column B absorber to be constructed in a follow-on project. The parametric study includes simulations on various design and operating parameters including the column height, solvent and gas flow inlet temperatures, location and cooling intensity of the intensified packing device, etc.

4.2 RESULTS

4.2.1 MFIX Simulations for Column A

For column A, CFD simulations with the MFIX solvent model have been performed using the matching operating conditions as outlined in Table 1. Temporal and spatial distributions of temperature, CO_2, and other species in solvent and gas are available from the simulation results, e.g., **Figure 14** shows snapshots of temperature and species distributions. **Figure 15** shows that the temperature profiles for the solvent and the gas in case #13 matched reasonably well with the experimental measurements. Note in the experiment, a total of four thermocouples were placed in the entire Column A.

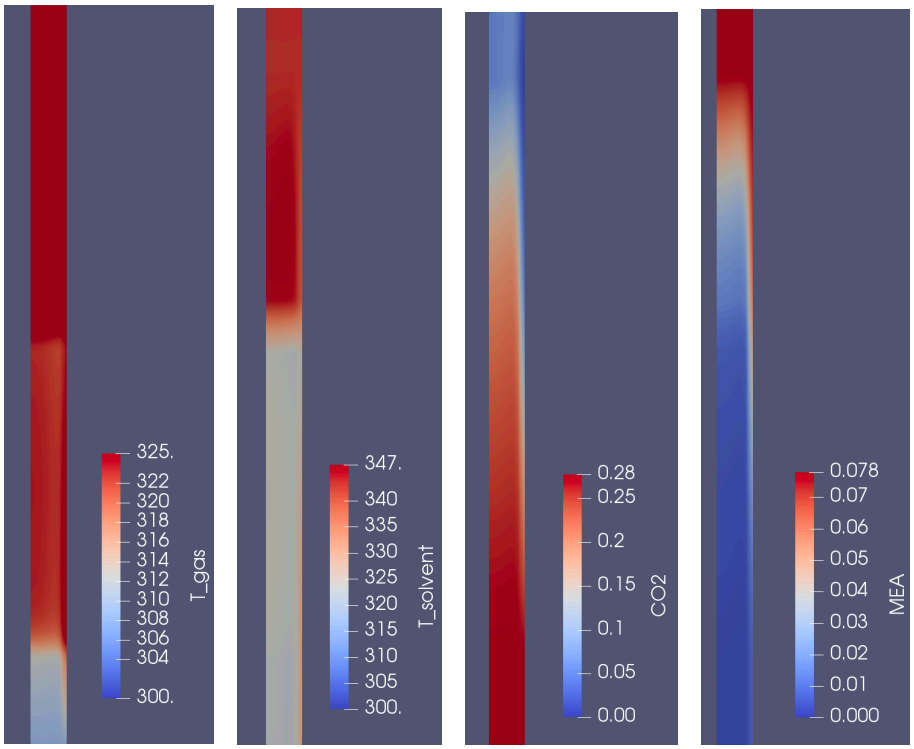

Figure 14. Illustration of two dimensional distributions of gas and solvent temperature (in K), CO_2, and MEA concentrations in the column.

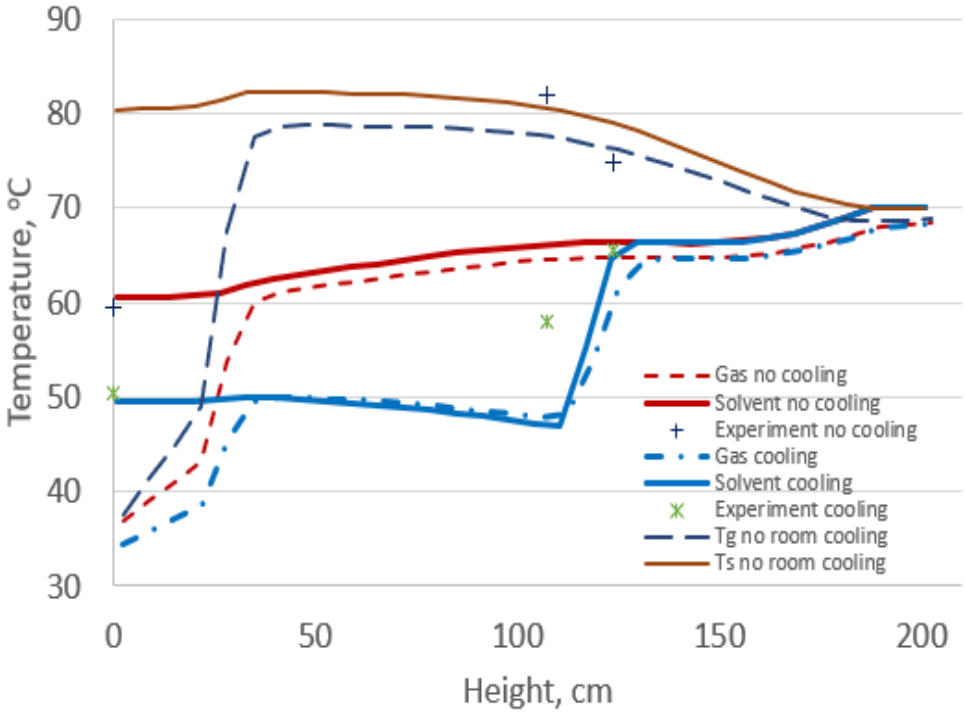

Figure 15.Temperature profile in Column A corresponding to case #14 in Table 4.

Overall, the calibration of the MFIX model with results from Column A for aqueous amine-based solvent looks promising, as the results predicted by the MFIX simulations agree qualitatively in terms of the effect of cooling on the CO_2 capture. The solvent model predicts that the cooling helps to improve the capture efficiency for all cases with 70ºC inlet solvent, and this is consistent with the experiment data. In general the model underpredicted the cooling benefit, especially when the CO_2 content is lower, as the solvent model predicts more complete CO_2 capture than measured from experiments even without the cooling.

One of the major reasons behind the discrepancy between the CFD prediction and the experiment data lies in the fact that MEA species composition was not the same for different testing cases because the MEA was regenerated differently after each case. Precise information on the initial inlet species concentrations is critical in calculating heat generation, thermal distribution, and CO_2 capture reactions. Since no species measurement was available from the experiments, the species concentration values were estimated and one fixed set of calibrated species concentration values was been used in all MFIX solvent model simulations. For reference, a similar calibration of MEA species contents was made in the AspenPlus based process model developed at WVU. Both the MFIX solvent model at ORNL and the process model at WVU derived the same conclusion: the regeneration of the MEA solvent between experiments was incomplete.

Table 4. Comparison of CO_2 capture efficiency between experiment and simulation results with both non-adiabatic and adiabatic conditions

#	Air Flow Rate (LPM)	CO_2 Flow Rate (LPM)	CO_2 Concentration (%)	Molar Capture Rate Before Cooling (mol/min)	Molar Capture Rate After Cooling (mol/min)	Fractional Increase (%)	Capture Efficiency (%) (Before Cooling → After Cooling)	MFIX non-adiabatic simulations	MFIX adiabatic simulations
11	810	90	10	2.24	2.30	2.7	59.9 → 61.2	72.9 → 73.1	66.8 → 73.2
10	510	90	15	2.75	2.90	5.5	73 → 77	74.2 → 75.4	67.1 → 74.7
9	360	90	20	2.95	3.29	11.5	78 → 88	79.8 → 82.2	72.0 → 80.7
8	264	90	25	3.52	3.57	4.3	94 → 98	94.0 → 95.9	84.3 → 94.6
14	360	40	10	1.38	1.45	5.1	83 → 87	99.4 → 99.3	99.2 → 99.2
13	360	63.5	15	1.53	1.77	15.7	58 → 67	96.8 → 97.0	93.2 → 97.2
9	360	90	20	2.95	3.29	11.5	78 → 88	79.8 → 82.2	72.0 → 80.7
12	360	120	25	3.07	3.28	6.9	62 → 66	62.3 → 65.4	54.0 → 63.1

4.2.2. Parametric study towards optimizing Column B design

CFD simulations have also been performed to identify the thermal bulge area and to sweep through the realistic design space, i.e., position of the intensified device and desired cooling capability, to identity the optimal location of the intensified device for different operating conditions for larger columns, and this activity has contributed to the design of Column B absorber.

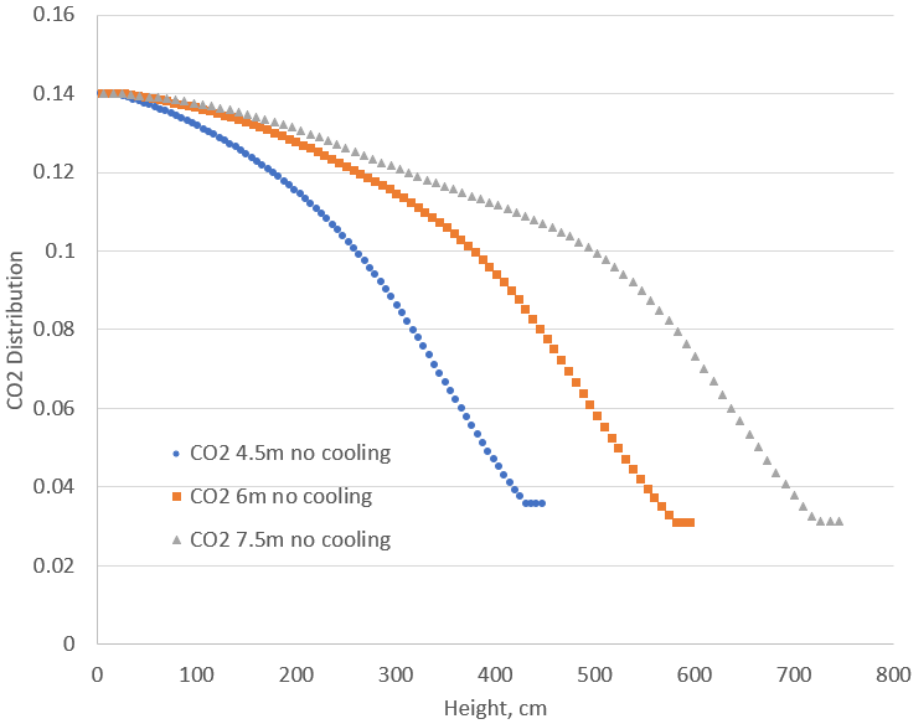

Figure 16. CO_2 distributions in columns with three different heights. All three columns share the same gas and solvent flowrates, inlet temperature, and species distributions.

The impact of column height on the CO_2 capture was tried first. With the same column diameter, three different column heights have been tried. As illustrated in **Figure 16**, for a specific set of operating conditions, the CO_2 capture efficiency increases as the column becomes taller, e.g., from 74.6% for 4.5 m column to 77.9% for a 7.5 m one. The impact is considered insignificant for the specific set of experimental conditions, and further increasing the column height has a diminishing return.

We then performed some parametric runs on different inlet temperature and different locations for the intensified packing device. A 12-inch-diameter 6-meter-tall column was chosen for the study, with gas flowrate of 3000 SLPM and 14% CO_2, and a solvent flowrate of 8 SLPM 25% MEA and 5% lean loading by mass. Two cooling sections are placed in the column, both 0.5 meter in height, one at 1.5 meter from the bottom, and a second one at 4.5 meters. Several different sets of inlet temperature values have been used in simulations for this parametric study and the results are recapped below

- 90ºC: capture improves from 53.8% to 81.6%
- 70ºC: capture improves from 68.4% to 82.6%
- 50ºC: capture improves from 76.9% to 81.7%
- 40ºC or lower: cooling hurts CO_2 capture efficiency

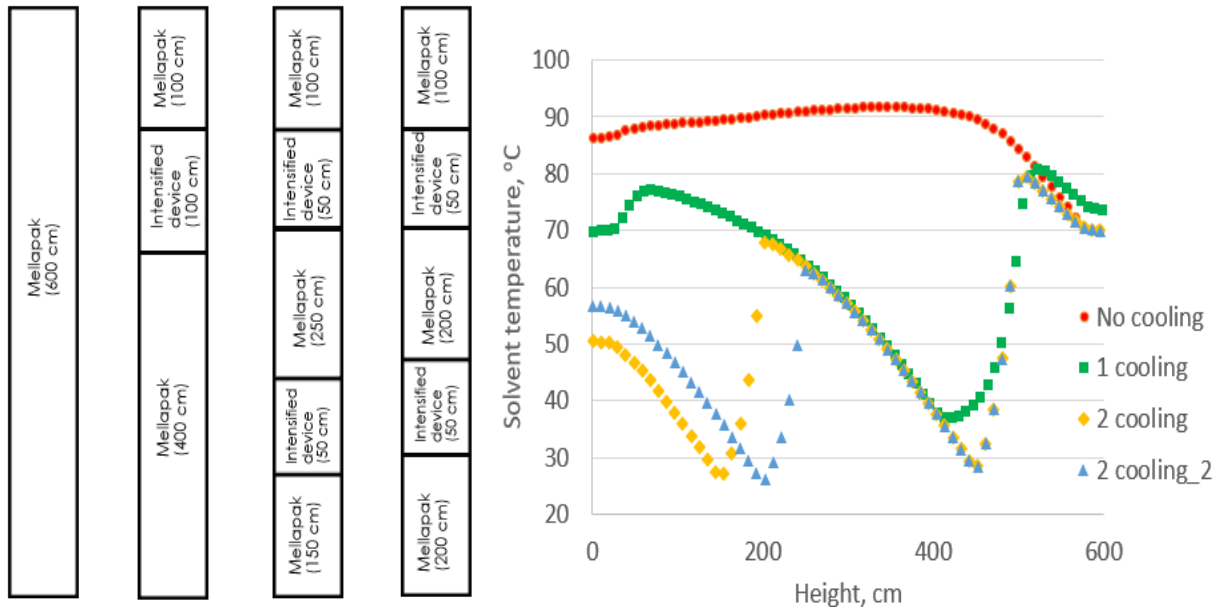

(a) (b)

Figure 17. Scouting runs to help column design in achieving the optimal cooling and CO_2 capture. (a) configurations of no cooling, one cooling section, two different two-cooling sections. (b) Temperature profiles for 4 different configurations, with both solvent and gas inlet temperature at 70°C.

The results shown in **Figure 17** and **Figure 18** also demonstrated that distributing the cooling in two locations is better than concentrating the cooling in one location, assuming the same total cooling capacity. If the inlet temperature is higher, placing the cooling closer to the inlet and thus reaping the benefit earlier is beneficial for the overall CO_2 capture efficiency, while delaying the cooling is preferred if inlet temperature is lower.

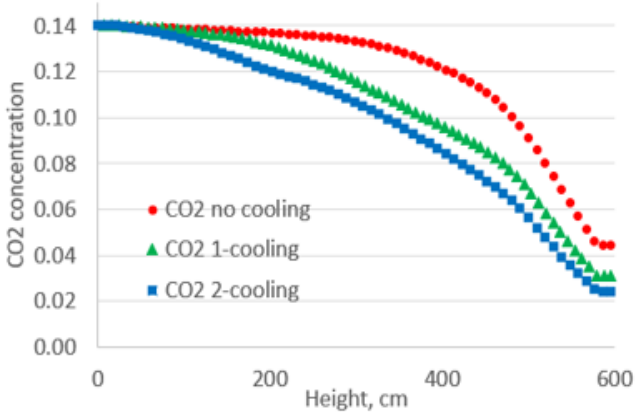

	CO_2 capture efficiency		
Inlet T (°C)	No cooling	One cooling	Two cooling
90	53.8%	76.9%	81.6%
70	68.4%	77.8%	82.6%

(a) (b)

Figure 18. (a) CO_2 concentration distributions and (b) CO_2 capture efficiencies for different cooling configurations.

A parametric study has also been performed on finding how much intra-stage cooling by the intensified device is optimal. As shown in **Figure 19**, the intra-stage cooling has a positive impact on improving CO_2 capture, and the improvement becomes more significant as the inlet temperature increases. More cooling helps, but the gain diminishes, especially for lower inlet temperatures.

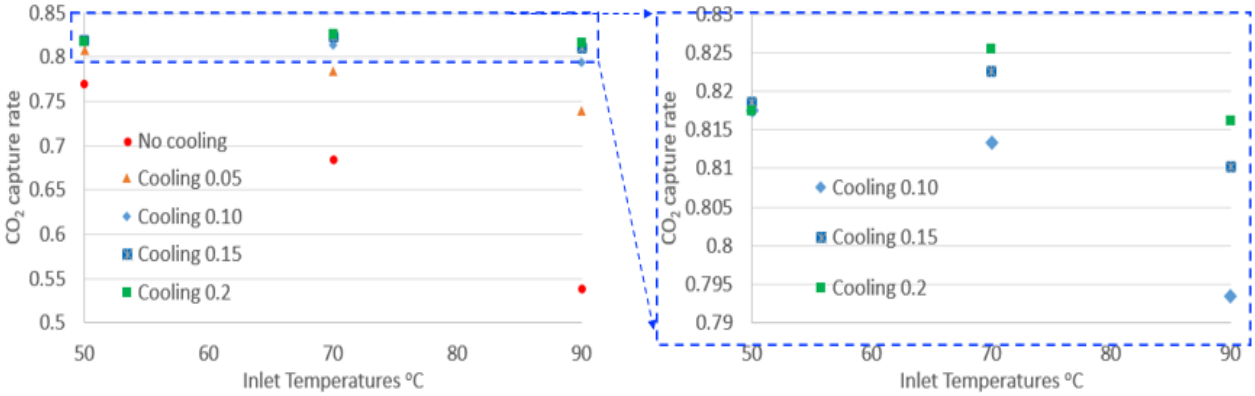

Figure 19. Capacity of cooling vs. CO_2 capture efficiency. A 12-inch-diameter 6-meter-tall column was chosen for the study, with gas flowrate of 3000 SLPM and 14% CO_2 and a solvent flowrate of 8 SLPM 25% MEA and 5% lean loading by mass.

Despite the achievements mentioned above, improvements on the solvent model are needed if it is to further quantitively analyze the performance of absorber and the cooling benefit. The most important improvement is to confirm the thermal calculations are correct. Without a correct thermal calculation, it is impossible to achieve a good prediction of the CO_2 capture. As mentioned above, there is large discrepancy between the solvent prediction and the experiment data on the temperature inside the absorber. The solvent model seems to have underreported the heat generated from the exothermic CO_2 capture reactions and, as a result, the maximum temperature bulge is not as large as measured in the experiments or predicted by WVU's AspenPlus-based process model. The small temperature bulge leads to underestimation of the cooling benefit. The thermal algorithm in the MFIX solvent model is built upon enthalpy calculations and, while the heat generation calculated by the 0-D model has been independently validated, some detailed analysis must be carried out to ensure that the heat generation and the changes of various species are consistent with each other in the 2D domain.

A couple of other improvements will also help. First an advanced thermal model on cooling by the intensified device could be beneficial. Currently the cooling model is very rudimentary as it is defined only by a constant coolant temperature and a fixed effective heat transfer coefficient for the entire region cooled with the intensified device. A more sophisticated model could refine the thermal calculation by considering the coolant flowrate, variation of the coolant temperature inside the intensified device, contact material between coolant and the column bed where MEA solvent and flue gas flow, etc. In addition, better coupling with low scale sub models, or more seamless utilizations of the results from the sub-models on many physics properties will also help improve the prediction. Currently, results from a limited number of sub-models have been

implemented in the device scale solvent model to provide those multi-physics properties such as contact angle, wetted surface, liquid hold up, drag, and mass transfer, and heat transfer.

5. CONCLUSIONS

Highly efficient CO_2 capture using LAS with intra-stage cooling has been demonstrated using an additively manufactured intensified packing device. The LAS was found to be a thermally sensitive solvent because of the lower heat capacity of the organic diluent compared with that of water, as well as the intrinsic thermodynamic behavior of the solvent. Based on a theoretical model, the highly efficient thermal management and its mass transfer enhancement were demonstrated using intra-stage cooling by the intensified packing device. A 15% temperature reduction and a fractional CO_2 capture enhancement of up to 25% were achieved. The performance of the LAS with respect to CO_2 capture was systematically investigated, and effects of solvent feed temperature, L/G mass flowrate ratio, and solvent regeneration were studied. Future work may be focused on better understanding the regeneration effects and long-term performance of the LAS with the goal to optimize the regeneration conditions and to balance the water content as an effective activator and as a diluent. The MFIX solvent model has been used to run simulations to predict the performance of Column A with aqueous amine-based solvents, and the results are compatible with the experiment data. CFD simulations have also been performed to identify the thermal bulge area and to sweep through the realistic design space, i.e., position of the intensified device and desired cooling capability, to identity the optimal location of the intensified device for different operating conditions for larger and taller columns, and this activity has contributed to the design of a Column B absorber. Additional work may also focus on optimizing the design of the intensified device to be more effective and reducing the length of column for a compact design for lower-concentration CO_2 gases, such as flue gas generated from natural gas combustion.

Overall, this work advances the technology towards a viable CO_2 capture process for point sources based on absorption by LAS. It has been shown that the performance of LAS is sensitive to temperature, and that the solvent temperature along the column needs to be kept lower than 45 ^oC for better CO_2 capture. The ORNL intensified packing device can be used to achieve this task, allowing for process intensification. Scaleup and optimization of the intensified device need to be investigated in future work.

6. ACKNOWLEDGMENTS

This research was funded by the Office of Fossil Energy of the US Department of Energy under project number FEAA375. Technical help by Mr. Scott Palko of the Applied Catalysis and Emissions Research Group of Oak Ridge National Laboratory is gratefully acknowledged. The authors are also thankful to Drs. Marty Lail and Paul Mobley of RTI International for providing the low-aqueous solvent for this study and also for helpful discussions. The report was edited by Ms. Olivia Shafer of ORNL and reviewed by Dr. Joanna McFarlane.